

01 Jan 2006

Completely Explosive Ultracompact High-Voltage Nanosecond Pulse-Generating System

Sergey I. Shkuratov

Evgueni F. Talantsev

Jason Baird

Missouri University of Science and Technology, jbaird@mst.edu

Millard F. Rose

et. al. For a complete list of authors, see https://scholarsmine.mst.edu/min_nuceng_facwork/1180

Follow this and additional works at: https://scholarsmine.mst.edu/min_nuceng_facwork

 Part of the [Explosives Engineering Commons](#)

Recommended Citation

S. I. Shkuratov et al., "Completely Explosive Ultracompact High-Voltage Nanosecond Pulse-Generating System," *Review of Scientific Instruments*, American Institute of Physics (AIP), Jan 2006.

The definitive version is available at <https://doi.org/10.1063/1.2168674>

This Article - Journal is brought to you for free and open access by Scholars' Mine. It has been accepted for inclusion in Mining Engineering Faculty Research & Creative Works by an authorized administrator of Scholars' Mine. This work is protected by U. S. Copyright Law. Unauthorized use including reproduction for redistribution requires the permission of the copyright holder. For more information, please contact scholarsmine@mst.edu.

Completely explosive ultracompact high-voltage nanosecond pulse-generating system

Sergey I. Shkuratov,^{a)} Evgueni F. Talantsev, and Jason Baird
Loki Inc., Rolla, Missouri 65409

Millard F. Rose and Zachary Shotts
Radiance Technologies, Inc., Huntsville, Alabama 35807

Larry L. Altgilbers
U.S. Army Space and Missile Defense Command, Huntsville, Alabama 35807

Allen H. Stults
U.S. Army Aviation and Missile Research, Development, and Engineering Center, Alabama 35898

(Received 30 October 2005; accepted 2 January 2006; published online 10 April 2006)

A conventional pulsed power technology has been combined with an explosive pulsed power technology to produce an autonomous high-voltage power supply. The power supply contained an explosive-driven high-voltage primary power source and a power-conditioning stage. The ultracompact explosive-driven primary power source was based on the physical effect of shock-wave depolarization of high-energy $\text{Pb}(\text{Zr}_{52}\text{Ti}_{48})\text{O}_3$ ferroelectric material. The volume of the energy-carrying ferroelectric elements in the shock-wave ferroelectric generators (SWFEGs) varied from 1.2 to 2.6 cm^3 . The power-conditioning stage was based on the spiral vector inversion generator (VIG). The SWFEG-VIG system demonstrated successful operation and good performance. The amplitude of the output voltage pulse of the SWFEG-VIG system exceeded 90 kV, with a rise time of 5.2 ns. © 2006 American Institute of Physics. [DOI: 10.1063/1.2168674]

I. INTRODUCTION

The development of autonomous compact pulsed power systems is important to the success of many scientific and engineering projects.¹ A novel type of autonomous explosive-driven pulsed power source, utilizing the electromagnetic energy stored for an infinite period of time in high-energy hard ferri- and ferromagnets, was recently developed.^{2–5} Operation of these devices is based on physical effects of shock-wave demagnetization of hard ferrimagnets² and ferromagnets.^{3–5} Miniature (9–25 cm^3 in volume) generators are capable of producing high-voltage pulses with amplitudes greater than 15 kV and high current pulses with amplitudes exceeding 4 kA. Piezoelectrics and ferroelectrics are another class of materials that are capable of storing electromagnetic energy for an almost infinite period of time. The design and performance of recently developed autonomous shock-wave pulsed power sources utilizing the electromagnetic energy stored in ferroelectric materials are described in Ref. 6. Compact explosive-driven generators based on shock-wave depolarization of ferroelectric energy-carrying elements have been demonstrated to be reliable and to have controllable electrical operation.^{6–8} The peak amplitudes of the electromotive force produced by ferroelectric generators are higher than those produced by shock-wave ferromagnetic generators.⁶ Therefore, it is a matter of great interest to develop combined pulsed power systems that utilize shock-

wave ferroelectric generators as the primary power source. In this work we successfully combined an explosive-driven shock-wave ferroelectric generator with a nonexplosive pulsed transformer (the spiral vector inversion generator⁹).

II. PRINCIPLES OF OPERATION AND EXPERIMENTAL TECHNIQUES

A schematic diagram illustrating the operation of the shock-wave ferroelectric generator (SWFEG) is in Fig. 1. This explosive-driven generator is based on the longitudinal (when the shock wave propagates along the polarization vector \mathbf{P}) shock-wave depolarization of ferroelectric materials. The energy-carrying elements in all the generators used in this work were poled lead zirconate titanate $\text{Pb}(\text{Zr}_{52}\text{Ti}_{48})\text{O}_3$ polycrystalline piezoelectric ceramic disks (supplied by EDO Corp.⁹) The parameters of the $\text{Pb}(\text{Zr}_{52}\text{Ti}_{48})\text{O}_3$ are density of $7.5 \times 10^3 \text{ kg/m}^3$, dielectric constant $\epsilon = 1300$, Curie temperature of 320 °C, Young's modulus of $7.8 \times 10^{10} \text{ N/m}^2$, piezoelectric constant $d_{33} = 295 \times 10^{-12} \text{ C/N}$, and piezoelectric constant $g_{33} = 25 \times 10^{-3} \text{ m}^2/\text{C}$.

Operation of the SWFEG is as follows. A shock wave, generated by high explosives, propagates through the ferroelectric disk and depolarizes it, releasing the induced charge to metallic contact plates on the ferroelectric disk. A pulsed electric potential (electromotive force, EMF) appears at that point on the high-voltage output terminals of the generator. The amount of electrical energy produced by SWFEG is determined by the quantity of electric charge released to the electrical circuit of the generator during explosive operation.

^{a)} Author to whom correspondence should be addressed; electronic mail: shkuratov@lokiconsult.com

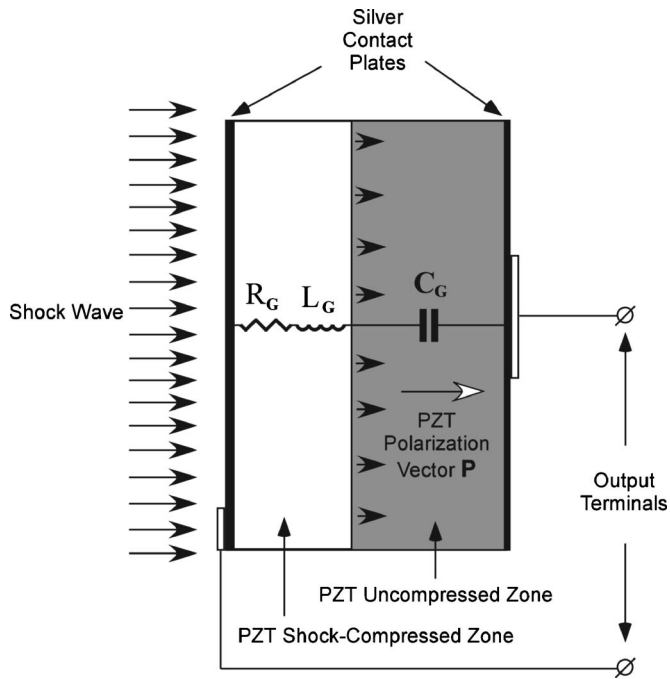


FIG. 1. Schematic diagram illustrating operation of the shock-wave ferroelectric generator. R_G and L_G are the resistance and inductance, respectively, of the shock-compressed zone of the ferroelectric energy-carrying element (through which the shock wave has already passed). C_G is the capacitance of the uncompressed zone (through which the shock wave has not passed).

The efficiency of this device depends on the degree of depolarization of the ferroelectric energy-carrying element under the action of a shock wave.

We performed an experimental investigation of the depolarization of a ferroelectric energy-carrying element within a compact SWFEG. It was shown⁸ that shock-wave compression of $\text{Pb}(\text{Zr}_{52}\text{Ti}_{48})\text{O}_3$ energy-carrying elements of the SWFEG by pressure in the range of 1.5–3.8 GPa caused practically complete depolarization of the ferroelectrics. The electric charge stored in the $\text{Pb}(\text{Zr}_{52}\text{Ti}_{48})\text{O}_3$ ferroelectric ceramic due to its remnant polarization is released within a time interval of 0.1–0.5 μs and can be transformed into pulsed power.

A schematic diagram of an explosive-driven high-voltage SWFEG is in Fig. 2. It contains a cylindrical body, an explosive chamber, an aluminum impactor, and a holder containing the ferroelectric module (the energy-carrying element). All the generators used in these experiments were charged with 14 g of desensitized RDX, a molecular high explosive, and the explosive was initiated by a RISI RP-501 exploding bridgewire detonator. Detailed information about the design of the SWFEG can be found in Ref. 6.

The vector inversion generator (VIG) is a pulse generator, which, as a single unit, can store an electric charge at 1 V and discharge it as a pulse having a peak value higher than the stored voltage.¹⁰ A schematic diagram of the VIG is in Fig. 2. The VIG contains two sheets of conductive material and two sheets of electrically insulating material arranged alternately and wound together into a roll, forming an open-ended transmission line. If we charge this rolled foil capacitor to voltage U_0 and then close the spark gap switch, the discharge generates an electromagnetic wave that originates

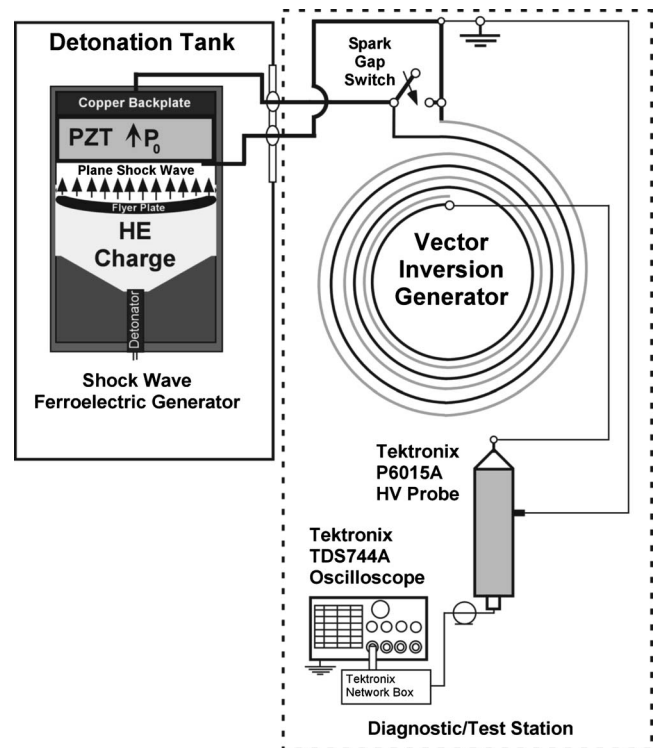


FIG. 2. Schematic diagram of a completely explosive SWFEG-VIG system.

from the switch and travels along the transmission line. As the wave travels, it converts the electrostatic field into an electromagnetic field and when it retraces its path after reflection at the end of the transmission lines, it converts the electromagnetic field back into an electrostatic field. An output pulse of amplitude $U_{\text{out}} = 2nU_0$ (n is a number of turns in the roll) and a rise time equal to double the electrical length of the transmission line appear at the contacts of the VIG. The advantages of this system are its simplicity and the short (nanosecond) rise time of the pulse it produces.

Explosive experiments were performed at the Rock Mechanics and Explosive Research Center at the University of Missouri-Rolla where we designed and constructed an experimental test stand to study explosive-driven pulsed power and microwave sources. Our main guideline for the design and development of this experimental test stand was to use commercial probes for monitoring the pulsed power signals. Out of several possibilities, we chose the design shown in Fig. 2. The setup has a detonation tank, where the explosive-driven generators are fired, and a diagnostic/test station.

The detonation tank is a cylindrical steel chamber that is 2.5 m in diameter and 7 m in length and its walls have a nominal 25.4 mm wall thickness. The tank is capable of withstanding nonfragmenting tests using up to 1 kg of high explosives. The explosive-driven generators tested are placed inside the detonation tank near a stainless-steel side port. The diagnostic/test station, containing probes, oscilloscopes, and other diagnostic and experimental equipments, is placed near the side port, but outside of the detonation tank. Some of generator output cables are connected to the diagnostic/test station through air-sealed connectors in the port. The other generator output cables are connected to the diagnostic/test station directly. In order to avoid mechanical strains being

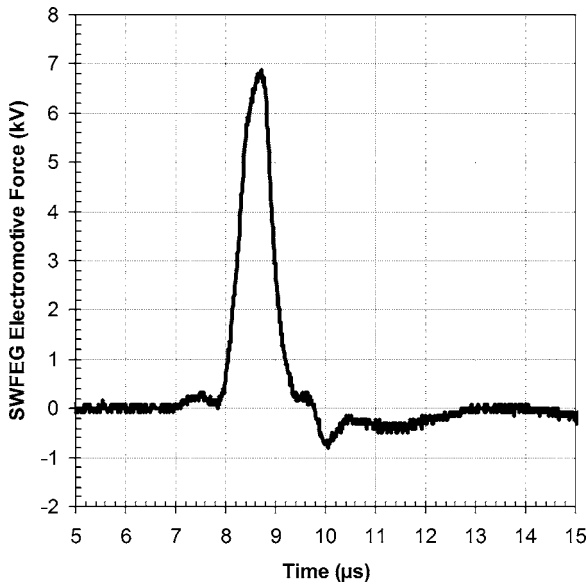


FIG. 3. Wave form of the pulsed electromotive force produced by a SWFEG operating in the open circuit mode. PZT energy-carrying element had dimensions of $D=27$ mm/ $h=2.1$ mm.

transmitted through the generator's output cables to the pulse measuring and recording systems during generator firing, the output cables are fixed in the port cover using specially developed cylindrical clamps. During explosive operation of the generator, the cables are cut off at their generator connections instead of at the measuring system connections. Since mechanical strains are not transferred to the diagnostic/test station through the cables, there is no mechanical effect from the explosive detonation on the results of the electrical measurements. Positioning the sensitive equipment outside the tank in this manner protects the equipment from the explosive environment within the tank, thereby preventing test-related damage.

A schematic diagram of the experimental setup used to test the SWFEG-VIG system is in Fig. 2. The SWFEG was placed inside the detonation tank. The output terminals of the SWFEG were connected to the input of the VIG. The negative terminal of the SWFEG was grounded. When fired, the SWFEG produced a positive high-voltage pulse that was applied to the input of the VIG spark gap switch. The output voltage of the completely explosive SWFEG-VIG system was monitored by a Tektronix P6015A high-voltage probe (rise time of 4 ns, resistance of 100 M Ω , capacitance of 3 pF) that was connected directly to the output of the VIG. All pulsed signals were recorded with Tektronix TDS744A (bandwidth of 500 MHz, 2 GS/s) and Tektronix TDS2024 (bandwidth of 200 MHz, 2 GS/s) oscilloscopes.

III. EXPERIMENTAL RESULTS

The first series of experiments was performed with SWFEGs containing $\text{Pb}(\text{Zr}_{52}\text{Ti}_{48})\text{O}_3$ ceramic disks of diameter $D=27$ mm and thickness $h=2.1$ mm. The wave form of a typical electromotive force pulse produced by a SWFEG operating in the open circuit mode is in Fig. 3. The EMF

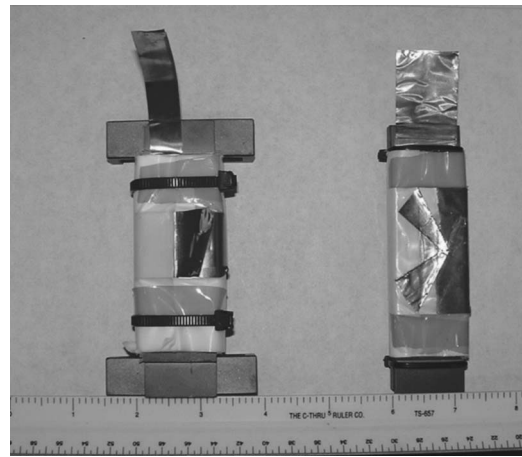


FIG. 4. Photo of the VIGs used in these experiments.

pulse amplitude was $U_g(t)_{\text{max}}=6.88$ kV, its full width at half maximum (FWHM) was 0.68 μs , and its rise time was $\tau=0.81$ μs .

The design and implementation of the VIG spark gap are mostly a matter of trial and error. A standard paper punch was used to make a repeatable hole in dielectric films, which could be stacked to lengthen the gap. In this way, the switch inductance was kept at a minimum and the breakdown voltage could be somewhat controlled. To get some idea of the impulse behavior of the gap, we developed a simple test fixture to allow an impulse to be applied to the switch ensemble.

The VIG chosen for the first experiments was an eight-turn unit made with a 0.1-mm-thick capacitor grade Teflon as the dielectric that had a width of 50.8 mm and with 0.05 mm copper shims as the capacitor conducting plates. These VIGs were wound on ferrimagnetic mandrels (ferrite 2535) with a width of 25.4 mm. The VIG had a "rectangular cross section," which did not affect its efficiency. The voltage efficiency (measured by voltage multiplication) of the devices was in the 80%–90% range. The calculated capacitance of these devices was approximately 8.9 nF. A photo of typical VIGs is in Fig. 4.

Operation of the SWFEG-VIG system is as follows. The explosive-driven SWFEG produces a microsecond pulse that impulse charges the VIG. When the charge voltage exceeds the VIG spark gap holdoff threshold, the VIG erects in a time equal to two wave transit times through the device (~ 6 ns), producing a transient voltage that is several times greater than the breakdown voltage of the VIG spark gap switch. Preliminary characterization of the VIG spark gap was done in the laboratory in real time, and the gap was tuned using a high-voltage dc power supply and was set to breakdown at approximately 3 kV.

The wave form of a typical high-voltage pulse produced by a SWFEG-VIG system is in Fig. 5. The peak voltage amplitude was $U(t)_{\text{max}}=28.8$ kV, its FWHM=20 ns, and its rise time was $\tau=6.75$ ns. The actual VIG charge voltage at the gap trigger point can be calculated from the spiral efficiency ($U_{\text{out}}=2nU_0$) and the output voltage. The unit triggered at about 2.6 kV. Even at voltages of only 28.8 kV, the

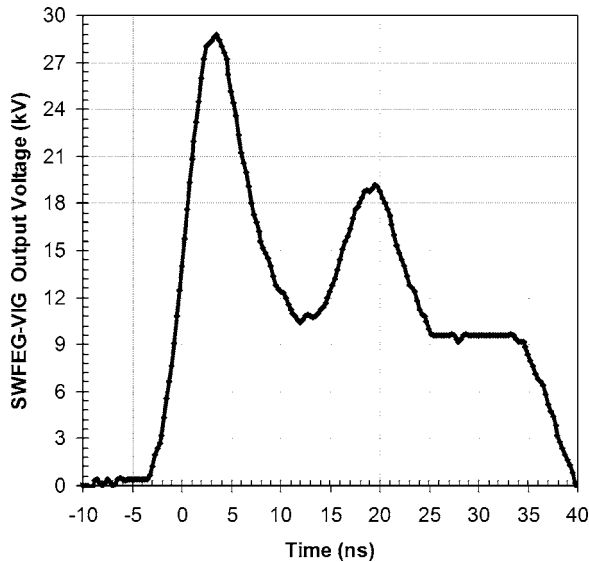


FIG. 5. Wave form of a typical high-voltage pulse produced by an explosive-driven SWFEG-VIG system. The SWFEG contained a PZT disk of dimensions $D=27$ mm/ $h=2.1$ mm. The VIG contained eight turns, and its spark gap breakdown voltage was 2.6 kV.

effects of corona in the VIG were appreciable and reduced the efficiency of the system to approximately 75%.

The next series of experiments was performed with SWFEGs containing PZT disks of dimensions $D=25$ mm/ $h=5.1$ mm. The pulsed EMF wave form produced by a SWFEG operating in the open circuit mode is in Fig. 6. The EMF pulse amplitude was $U_g(t)_{\max}=16.7$ kV, FWHM $=0.99$ μ s, and $\tau=1.02$ μ s.

In this series of experiments, we used a five-turn VIG. The device was prepared similar to the eight-turn unit (see description above), but was oil impregnated to eliminate corona effects and was capable of producing output voltages in excess of 100 kV. The calculated capacitance of the VIG was on the order of 5.6 nF. The breakdown voltage of the VIG spark gap was once again tuned to trigger at a set voltage using a high-voltage dc power supply to ensure that the unit

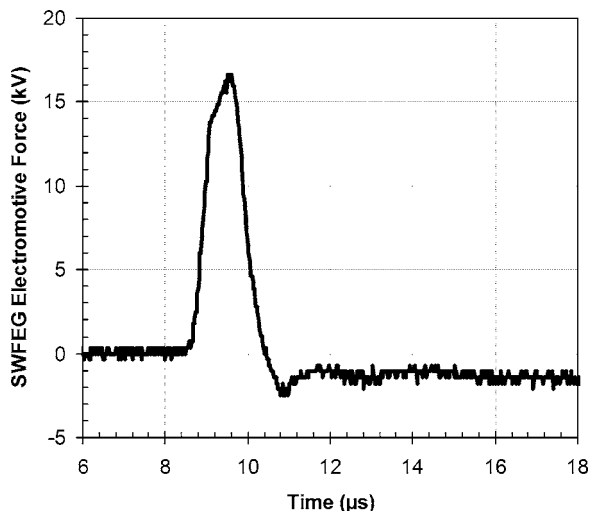


FIG. 6. Wave form of the pulsed electromotive force produced by a SWFEG operating in the open circuit mode. PZT energy-carrying element had dimensions of $D=25$ mm/ $h=5.1$ mm.

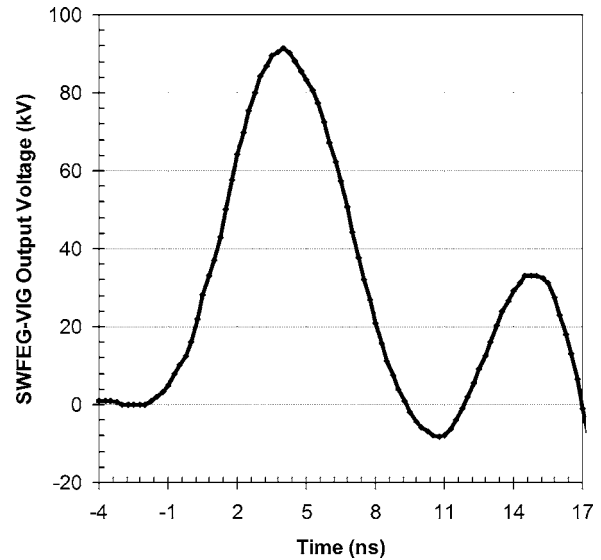


FIG. 7. Wave form of a typical high-voltage pulse produced by an explosive-driven SWFEG-VIG system. The SWFEG contained a PZT disk of dimensions $D=25$ mm/ $h=5.1$ mm. The VIG contained five turns. The VIG spark gap breakdown voltage was 11.1 kV.

would discharge at the appropriate time. The spark gap spacing was set to dc discharge at approximately 6 kV, expecting that it would probably be more than that under impulse conditions. The experimental setup for this series of tests was similar to that in the previous series (Fig. 2). The only difference was that we used a custom voltage divider with a coefficient of 5.02 connected to the Tektronix P6015A high-voltage probe.

The wave form of a typical high-voltage pulse produced by a SWFEG-VIG system is in Fig. 7. The peak voltage amplitude was $U(t)_{\max}=91.4$ kV, FWHM $=6.5$ ns, and $\tau=5.25$ ns. The rise time of the pulse approached the resolution limit of the Tektronix high-voltage probe. Probe resolution, as well as stray capacitive effects, may distort the rise time of the SWFEG-VIG system and introduce considerable rise-time error. The calculated rise time for this system was on the order of 4 ns. The unit triggered at approximately 11.1 kV, which was almost twice the level at which the spark gap switch was set to break under dc conditions.

We have demonstrated successful operation of an autonomous completely explosive high-voltage pulsed power system using an explosive-driven SWFEG as the primary power source with a VIG as a power-conditioning stage. Adding a VIG stage increases the voltage output of the SWFEG by a multiplication factor depending on the VIG's parameters, while simultaneously compressing the pulse width into the range of a few nanoseconds. This combination produces an extremely high-power, single-shot pulser.

¹L. L. Altgilbers, M. D. J. Brown, I. Grishnaev, B. M. Novac, I. R. Smith, I. Tkach, and Yu. Tkach, *Magnetocumulative Generators* (Springer-Verlag, New York, 2000).

²S. I. Shkuratov, E. F. Talantsev, J. C. Dickens, and M. Kristiansen, *J. Appl. Phys.* **91**, 3007 (2002).

³S. I. Shkuratov, E. F. Talantsev, J. C. Dickens, and M. Kristiansen, *Rev. Sci. Instrum.* **73**, 2738 (2002).

⁴S. I. Shkuratov, E. F. Talantsev, J. C. Dickens, and M. Kristiansen, *J. Appl. Phys.* **92**, 159 (2002).

- ⁵S. I. Shkuratov, E. F. Talantsev, J. C. Dickens, M. Kristiansen, and J. Baird, *Appl. Phys. Lett.* **82**, 1248 (2003).
- ⁶S. I. Shkuratov, E. F. Talantsev, L. Menon, H. Temkin, J. Baird, and L. L. Altgilbers, *Rev. Sci. Instrum.* **75**, 2766 (2004).
- ⁷Y. Tkach, S. I. Shkuratov, E. F. Talantsev, M. Kristiansen, J. Dickens, L. L. Altgilbers, and P. T. Tracy, *IEEE Trans. Plasma Sci.* **30**, 1665 (2002).
- ⁸S. I. Shkuratov, E. F. Talantsev, J. Baird, H. Temkin, L. L. Altgilbers, and A. H. Stults, *Proceedings of 14th APS Topical Conference on Shock Compression of Condensed Matter*, Baltimore, 2–5 August 2005 (unpublished).
- ⁹EDO Electro-Ceramic Products Inc., 2645 South 300 West, Salt Lake City, UT 84115, www.edoceramic.com
- ¹⁰S. A. Merryman, F. Rose, and Z. Shotts, *14th IEEE International Pulsed Power Conference, 2003*, Digest of Technical Papers (PPC-2003, Los Alamitos, CA, Vol. 1, pp. 249–252).